

Article

Modification of Hybrid Receptor Model for Atmospheric Fine Particles (PM_{2.5}) in 2020 Daejeon, Korea, Using an ACERWT Model

Sang-woo Han ¹, Hung-soo Joo ², Kyoung-chan Kim ², Jin-sik Cho ¹, Kwang-joo Moon ³ and Jin-seok Han ^{2,*}¹ E2M3 Inc., Anyang 14059, Republic of Korea; white8703@e2m3.com (S.-w.H.)² Department of Environmental Engineering, Anyang University, Anyang 14028, Republic of Korea; hungsoo.joo@gmail.com (H.-s.J.)³ National Institute of Environmental Research, Incheon 22689, Republic of Korea; iamian@korea.kr

* Correspondence: nierhan@hanmail.net; Tel.: +82-031-463-1292

Abstract: Hybrid receptor models overestimate the contribution of background areas (no specific emission sources), like the Yellow Sea in Korea. This study aimed to improve model performances using Advanced Concentration Emission and Retention Time Weighted Trajectory (ACERWT). ACERWT was combined with a positive matrix factorization (PMF), back trajectory, and Regional Emission Inventory in Asia (REAS). The PMF receptor model used one year of data from Korea's Central Air Environment Research Center. In the PMF receptor model, eight sources (dust/soil, secondary nitrate, biomass burning, vehicles, secondary sulfate, industry, coal combustion and sea salt) influenced PM_{2.5} pollution at the receptor site (Daejeon, Korea). Secondary sulfate was the most dominant source, followed by secondary nitrate and vehicle sources. ACERWT results showed high contributions from China, Japan, and Korean regions, while the contribution from the Yellow Sea was significantly lower. Several regions, such as the eastern and south-eastern areas of China, the southern area of Taiwan, the western area of Tokyo, and the central area of Korea, showed high contributions due to large-scale emission facilities and industrial complexes. In this study, the ACERWT model significantly improved its performance regarding regional contributions to PM_{2.5} pollution at the receptor site.

Keywords: PM_{2.5}; positive matrix factorization; emission source; advanced concentration emission and retention time-weighted trajectory; hybrid receptor model



Citation: Han, S.-w.; Joo, H.-s.; Kim, K.-c.; Cho, J.-s.; Moon, K.-j.; Han, J.-s. Modification of Hybrid Receptor Model for Atmospheric Fine Particles (PM_{2.5}) in 2020 Daejeon, Korea, Using an ACERWT Model. *Atmosphere* **2024**, *15*, 477. <https://doi.org/10.3390/atmos15040477>

Academic Editor: Nicolas Moussiopoulos

Received: 30 January 2024

Revised: 27 March 2024

Accepted: 9 April 2024

Published: 12 April 2024



Copyright: © 2024 by the authors. Licensee MDPI, Basel, Switzerland. This article is an open access article distributed under the terms and conditions of the Creative Commons Attribution (CC BY) license (<https://creativecommons.org/licenses/by/4.0/>).

1. Introduction

The region of East Asia emits a large amount of air pollutants owing to its high population density, industrial activities, and energy consumption [1]. Thus, various challenges in this region have been tried to identify high-concentration events and significant emission sources of fine particles (PM_{2.5}) [2]. A dispersion model based on pollution sources was used earlier in the year. Receptor models have been developed to overcome some limitations of the earlier dispersion models and have been recognized as a valuable tool in air pollution modeling [3]. Since chemical element balance (CEB) was presented by Miller et al. (1972), receptor models have been continuously developed and upgraded up to now [4].

Paatero (1997) studied using various methods to find out the effect of fine particles at the receptor site and tried to calculate the relationship between the generation sources and concentrations of fine particles. Eventually, the positive matrix factorization (PMF) model was developed to estimate the source profile and mass contribution of fine particles [5]. Many studies using the PMF receptor model have been conducted to discover primary sources and regions (or areas) contributing to receptor sites. Recently, hybrid receptor models have been actively applied in East Asia to track source locations to receptor sites [2,6–12]. Most studies using the hybrid receptor model in Korea focused on the source apportionment

of PM_{2.5} concentration in the capital and background areas [2,7,11,12]. Recently, various trials were carried out to identify information about the source location. Linkage analysis with a back trajectory model has been frequently used for tracing source locations [6–12].

Owing to the fact that the PMF receptor model has limitations in identifying the source location, hybrid receptor models, which are a combined PMF receptor model and back trajectory models of air masses, have been frequently studied, e.g., Potential Source Concentration Function (PSCF), Concentration Weight Trajectory (CWT) and Residence Time Weight Concentration (RTWC) [13–15]. However, these models tend to show the contribution of PM_{2.5}, especially in regions with no emission source (i.e., ocean areas), to be unexpectedly high [16,17]. Several hybrid receptor models developed to overcome this limitation still lack information on source locations [18–23] and need improvement.

In our previous study using the CWT model (modified CWT model, MCWT), we tried to improve the limitation of the regional contribution of the hybrid receptor model caused by overlapping several air masses. Although the contribution of the Yellow Sea to the receptor site in the MCWT model was lowered, the result of the Yellow Sea contribution was still high and should be complemented [24]. Therefore, as an improvement of the hybrid receptor model, which identifies primary sources and regional contributions to the receptor site, in this study, the Advanced Concentration, Emission, and Retention Time Weighted Trajectory (ACERWT) model was newly introduced and used to identify source locations and those contributions more clearly to the receptor site.

Moreover, it can be expected that the approach introducing the ACERWT model in this study has a significant benefit in figuring out the PM_{2.5} contributions of surrounding regions on a large scale.

2. Experiment Method

2.1. Sampling Location and Monitoring Site

The monitoring site was one of the supersites (Central Air Environment Research Center), which was located in the central region of Korea in the Daejeon Metropolitan region (36°19′21.4″ N (latitude), 127°24′49.7″ E (longitude)). The location of the monitoring site is described in Figure 1.

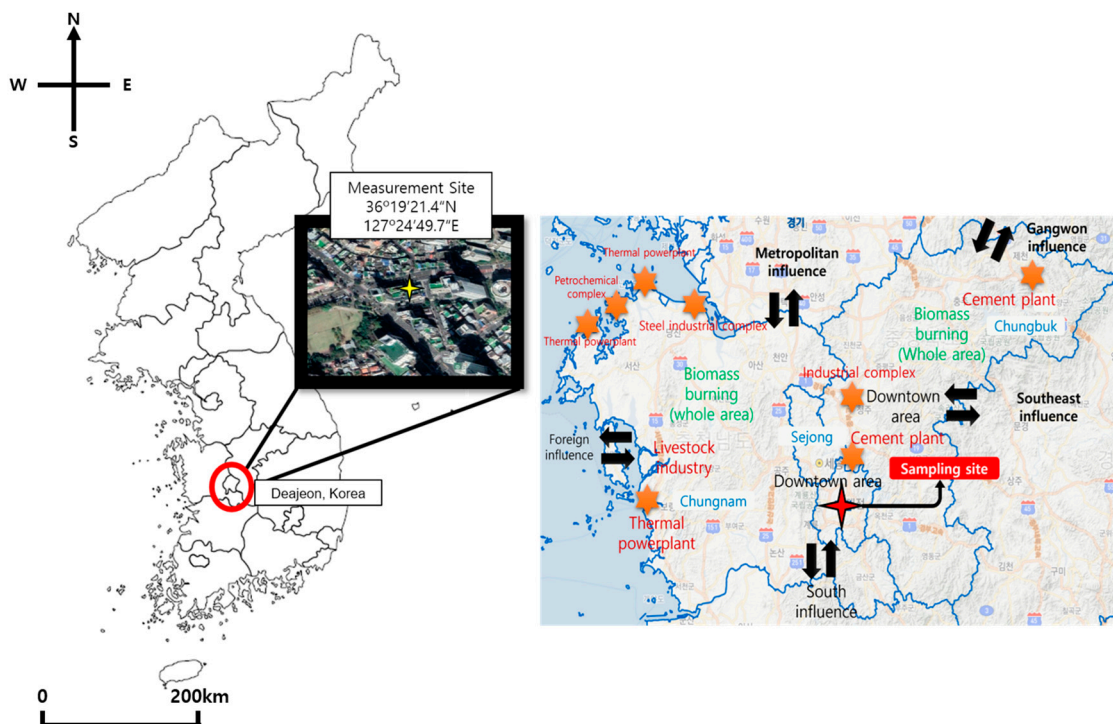


Figure 1. Location of the sampling and monitoring site (star symbol) [24].

Daejeon metropolitan region is one of the critical regions for interpreting Korea's national air pollution. This region is located in the center of Korea. Thus, it is surrounded by the capital region (north), large industrial complexes (west), and agricultural areas (south), and these surrounding regions influence the air pollution in this area.

2.2. Sampling and Data Analysis

This study used one year of full measurement data from the Central Air Environment Research Center. Measurement parameters of PM_{2.5} are mass concentration, eight ions (SO₄²⁻, NO₃⁻, Cl⁻, Na⁺, NH₄⁺, K⁺, Mg²⁺, Ca²⁺), organic carbon (OC), elemental carbon (EC), and 17 heavy metals (Si, S, K, Ca, Ti, V, Cr, Mn, Fe, Ni, Cu, Zn, As, Se, Br, Ba, and Pb). PM_{2.5} mass concentration was measured in real-time by a BAM-1020 (Met One Ins., Grants Pass, OR, USA), and ions were measured by an AIM-9000D (AIM, URG Co., Chapel Hill, NC, USA) [25,26] and those lower detection limits were 0.0008~0.008 µg/m³. Carbonaceous compounds (OC and EC) were measured by a Sunset OC/EC analyzer using the thermal/optical transmittance (TOT) method (OCEC Aerosol Analyzer, Sunset Laboratory Inc., Oregon, USA). Those detection limits were 0.2 µg/m³ for OC and 0.0007 µg/m³ for EC, respectively. Table 1 shows the gas and temperature conditions of the carbon analyzer [25]. Heavy metals were analyzed by an Online XRF (Xact[®] 625i, SailBri Cooper, Inc., Tigard, OR, USA).

Table 1. Gas/temperature conditions of the TOT analyzer.

Program Activity	Carrier Gas	Ramp Time (Second)	Program Temperature
Oven Purge	Helium	10	1
1stRamp	Helium	70	310
2edRamp	Helium	60	480
3rdRamp	Helium	60	615
4thRamp	Helium	90	840
-	Helium	30	0
1stRamp	O ₂ /Helium	35	550
2ndRamp	O ₂ /Helium	105	850
Internal			
Std. Calibration	CH ₄ /Helium	120	0
Cool down	Helium	1	0

The mass concentration of 17 elements was detected by the non-destructive analysis method. Further details on sampling and analysis methods are provided in the references [25,27]. Uncertainties of measurement data were examined by the procedure of the PMF receptor model [27] and Equation (1), i.e., the elimination of missing values, chemical species with low reliability, signal-to-noise ration < 0.2, measurement detection limits (MDL), and so on. Table 2 shows the measurement detection limits of PM_{2.5} components.

$$\sqrt{(\text{error fraction} \times \text{concentration})^2 + (0.5 \times \text{MDLs})^2} \quad (1)$$

2.3. Positive Matrix Factorization (PMF)

Concentration data of PM_{2.5} components were used in the PMF receptor model to trace primary emission sources at the receptor site. The PMF receptor model was operated using the methods reported in the 2020 Annual Intensive Air Quality Monitoring Station report by the National Institute of Environmental Research (NIER) [27]. Input and uncertainty data were pre-treated using concentration data and the standard errors of PM_{2.5} components. Finally, the total input data was 5257, used in the PMF receptor model.

Table 2. MDL of PM_{2.5} components.

	Components	MDL		Components	MDL	Components	MDL
Ions	SO ₄ ²⁻	0.00595	Elements	Si	0.03690	Cu	0.00022
	NO ₃ ⁻	0.01018		S	0.00515	Zn	0.00019
	Cl ⁻	0.00966		K	0.00309	As	0.00016
	Na ⁺	0.00328		Ca	0.00069	Se	0.00021
	NH ₄ ⁺	0.00218		Ti	0.00036	Br	0.00025
	K ⁺	0.04444		V	0.00034	Ba	0.00088
	Mg ²⁺	0.00106		Cr	0.00025	Pb	0.00030
	Ca ²⁺	0.00286		Mn	0.00032		
Carbons	OC	0.29731	Fe	0.00042			
	EC	0.00084	Ni	0.00024			

2.4. Emission Inventories

Regional Emission Inventory in Asia (REAS) version 3.2, provided by the National Institute for Environmental Science (NIES) in Japan, was used as East Asia’s air pollution emission data. This emission inventory was updated by Kurokawa et al. in 2020, and it included the real emission data set of East-North Asia from 1950 to 2015 [28]. This emission inventory was composed of 10 parameters (SO₂, NO_x, CO, NMVOC, PM₁₀, PM_{2.5}, BC, OC, NH₃, and CO₂) and seven sources (power plant, industry, transportation, domestic fuel combustion, industrial process, agriculture, etc. (suspended emission, solvent use, and human being). Monthly emission data were obtained with a 0.25 × 0.25 latitude and longitude resolution.

2.5. Advanced Concentration, Emission, and Retention Time-Weighted Trajectory (ACERWT)

The CWT model is frequently applied in the related analysis of the hybrid receptor model in Korea. The CWT model expresses the regional contributions using the weighted trajectories of input air masses based on air pollutant concentration at the receptor site. The equation of CWT is shown in Equation (2).

$$CWT_{i,j} = \frac{\sum_{l=1}^L C_l \tau_{i,j,l}}{\sum_{l=1}^L \tau_{i,j,l}} \tag{2}$$

CWT_{*i,j*} means the model results at the grids *i* (latitude), *j* (longitude), C_{*l*} is the concentration (µg/m³) when trajectory *l* reaches the receptor site, τ_{*i,j,l*} is the retention time of trajectory *l* in the grid (*i,j*). The CWT model has a limitation of overestimation in some grids owing to the overlapping of several trajectories [24]. Thus, a weighted method in concentrations and emissions was tried to overcome this limitation.

ACERWT model is the combination method using each grid’s emission data of East-North Asia and the CWT method. As the first step in ACERWT, the emissions at the grid (*i,j*) which *l* trajectory passes are estimated as like Equation (3) [24].

$$C_{k,l} = \frac{S_{k,l}}{\sum_{k=1}^{N_l} S_{k,l}} = C_l \frac{S_{k,l}}{S_l} \tag{3}$$

C_{*k,l*} means the concentration considered the emission data and its weighting factor at the receptor site for *l* trajectory. *k* is the area where *l* trajectory passes, S_{*k,l*} is the emissions at the *k* area in the *l* trajectory. N_{*l*} is the total number of *k* in the trajectory *l*, S_{*l*} is the total emission on the trajectory *l*. As the second step, Equation (4) shows the calculation of the ACERWT model result.

$$ACERWT_{i,j} = \frac{\sum_{l=1}^M \sum_{k=1}^{N_l} C_{k,l} \tau_{i,j,k,l}}{\sum_{l=1}^M \sum_{k=1}^{N_l} \tau_{i,j,k,l}} \tag{4}$$

$ACERWT_{i,j}$ is the relative contribution of $PM_{2.5}$ concentration to the receptor site at the grid (i, j) . $\tau_{i,j,k,l}$ is used as the retention time at the k area contained in the grid (i, j) on the l trajectory.

Figure 2 shows the flow chart of the ACERWT model. ACERWT is the combination model to identify the regional contribution to the receptor site, PMF receptor model, HYSPLIT (back trajectory), and emission inventory. The size of the grid was 1° and the region of Korea was located in the center of Northeast Asia.

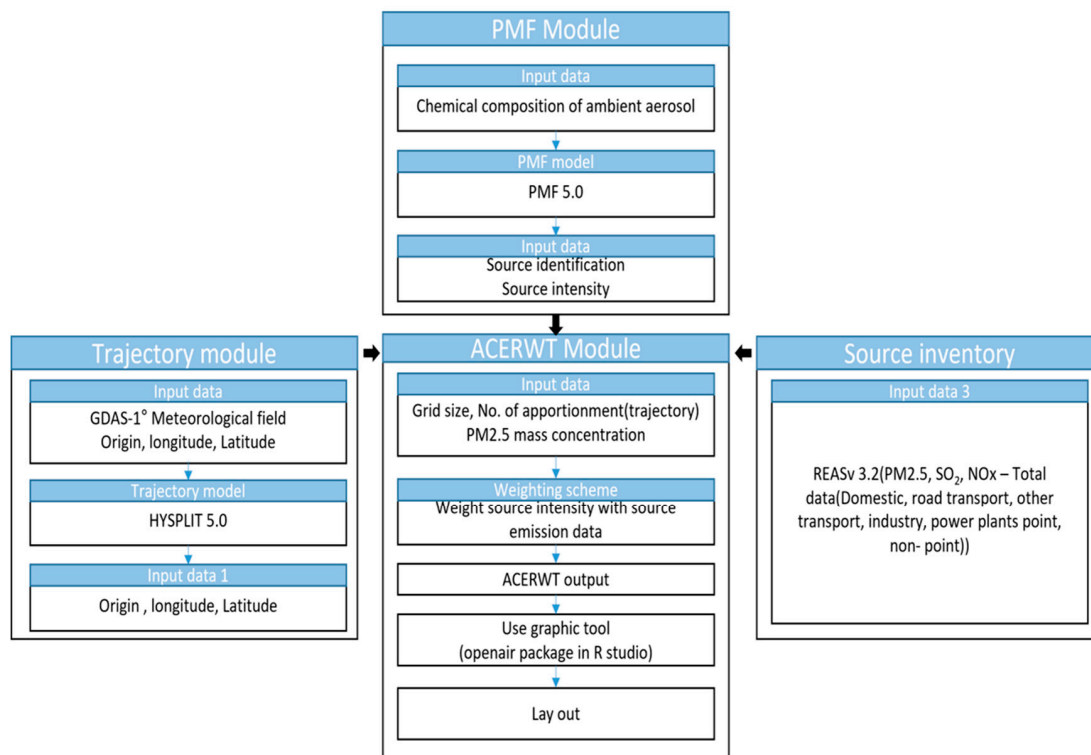


Figure 2. Flow chart of the ACERWT model applied to this study.

3. Results and Discussions

3.1. Emission Inventory

To figure out the regional source contribution of major sources in the grids of the ACERWT model, Figure 3 shows the summated emissions of $PM_{2.5}$, SO_x and NO_x for vehicles, industries, coal combustions, and the total source in East Asia. The contribution of vehicle sources is higher than that of other sources in Korea. At the same time, the contributions of industrial and coal combustion_domestic (residential coal combustion) sources are higher in China. Mainly, coal combustion sources for power plants are concentrated in the Sandung Peninsula, near Korea.

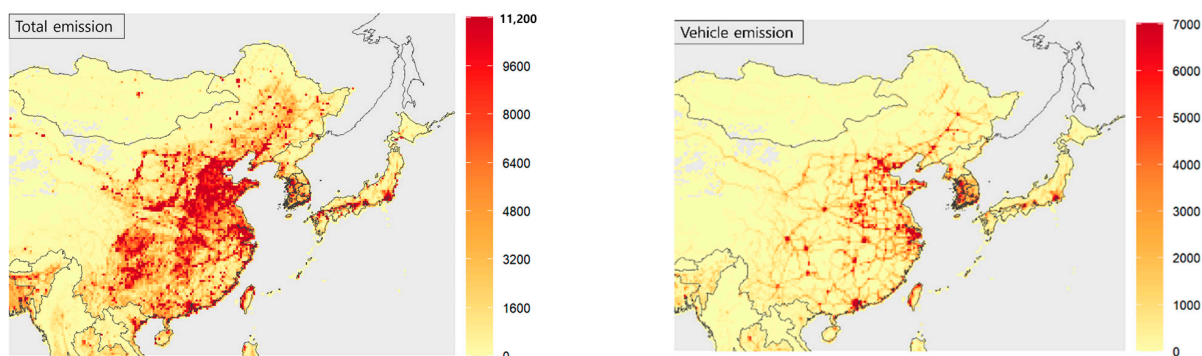


Figure 3. Cont.

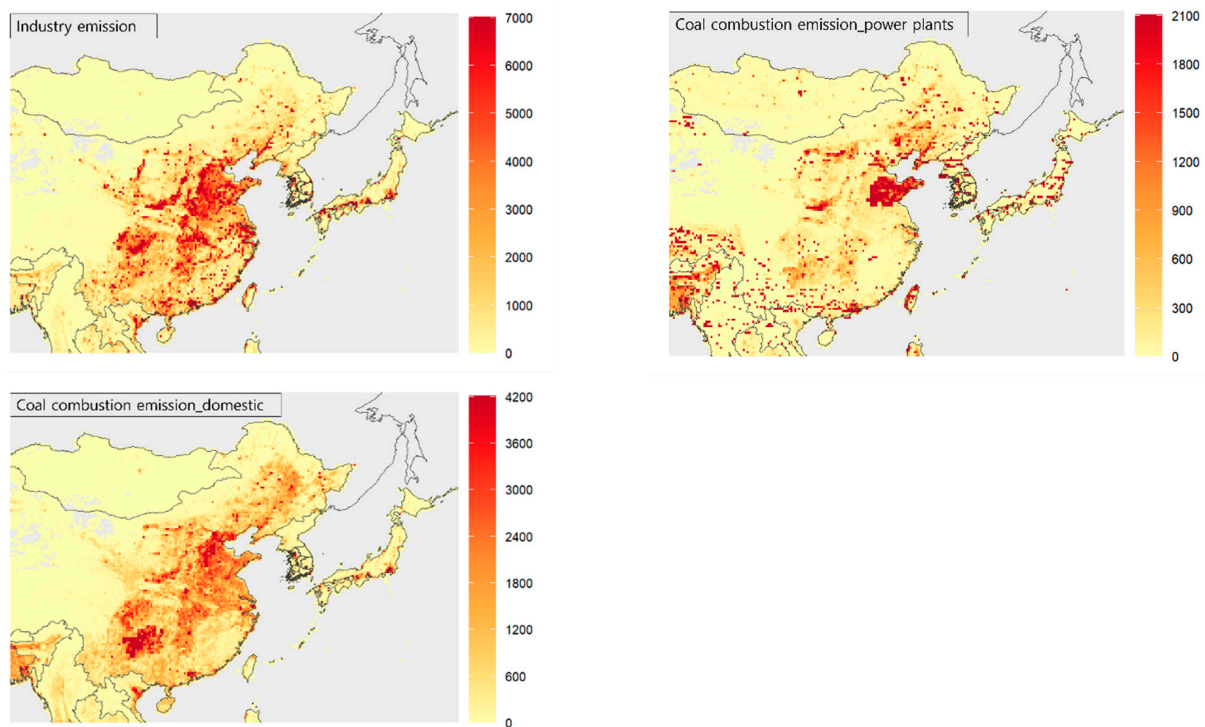


Figure 3. Summated emission of PM_{2.5}, SO_x and NO_x in East Asia region (2020).

3.2. Chemical Composition of PM_{2.5}

Table 3 shows the concentrations of chemical species of PM_{2.5}. PM_{2.5} concentrations were $22.2 \pm 15.3 \mu\text{g}/\text{m}^3$ in the measurement periods, and the maximum concentration was reached by $104 \mu\text{g}/\text{m}^3$. Fractions of ions, carbonaceous compounds, and heavy metals are 51%, 22%, and 12%, respectively.

Table 3. Average concentrations of chemical species (PMF input data) during the measurement period ($\mu\text{g}/\text{m}^3$).

	AVG.	MAX.	MIN.	STD.	Sample No.
PM _{2.5}	22.1	104	1	15.4	8460
SO ₄ ²⁻	3.75	15.9	0.06	2.47	6244
NO ₃ ⁻	5.52	46.5	0.01	6.42	6258
Cl ⁻	0.31	5.07	0.01	0.35	6257
Anion	9.56	58.2	0.11	7.92	8693
Anion/PM _{2.5}	0.38	0.81	0.06	0.20	8693
Na ⁺	0.15	2.62	0.01	0.17	6255
NH ₄ ⁺	2.91	17.9	0.01	2.55	6258
K ⁺	0.15	1.14	0.01	0.12	6050
Mg ²⁺	0.02	0.95	0.01	0.04	6218
Ca ²⁺	0.11	2.27	0.01	0.15	6223
Cation	3.30	18.2	0.05	2.67	8693
Cation/PM _{2.5}	0.002	0.07	0.0001	0.006	8785
Ion/PM _{2.5}	0.51	0.99	0.04	0.27	8693
OC	3.42	16.1	0.27	2.05	7367
EC	0.95	4.69	0.02	0.58	7367
Carbon	4.38	19.2	0.46	2.85	8744
Carbon/PM _{2.5}	0.22	0.97	0.04	0.12	8744
Metal	2.41	10.4	0.06	1.66	8780
Metal/PM _{2.5}	0.12	0.86	0.01	0.06	8780

Figure 4 and Table 4 show the fractions of chemical species depending on PM_{2.5} concentration level and frequencies depending on PM_{2.5} concentration level by season. NO₃⁻ and NH₄⁺ increased with increasing PM_{2.5} concentration, and high concentrations of PM_{2.5} were frequently observed during the winter. This means that the formation of secondary aerosols such as (NH₄)₂SO₄ and NH₄NO₃ actively progressed with increasing PM_{2.5} concentration, especially the formation of NH₄NO₃, which was more active in winter. Guo et al. 2010 reported that the reaction of NH₄NO₃ ↔ HNO₃ + NH₃ could be well progressed by the heterogeneous reaction with temperature conditions [29]. In addition, ammonia concentration at 2021 Daejeon was high in the winter season, and the formation of NH₄NO₃ progressed well owing to heterogeneous reactions in our recent study [30]. Sulfate (SO₄²⁻) and OC are well-known pollutants of long-range transportation and vehicle emissions, respectively. The contribution to high PM_{2.5} concentration by these two species was not higher than NO₃⁻. The nitrate effect mainly caused the high PM_{2.5} concentrations.

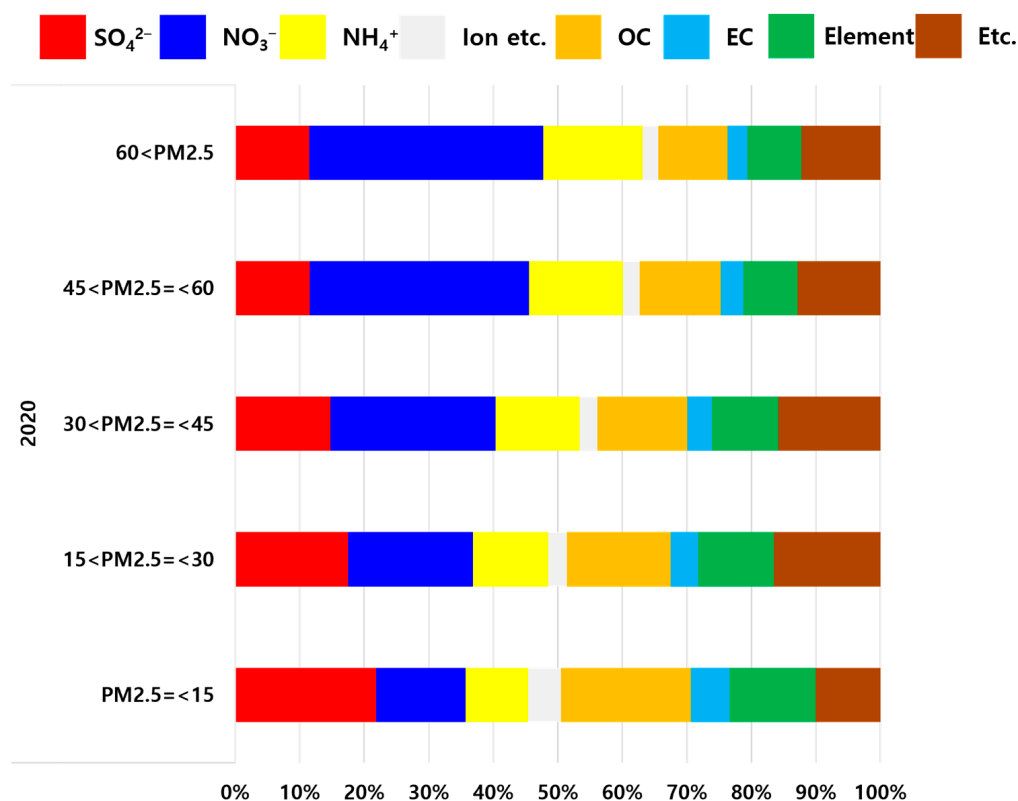


Figure 4. Fractions of chemical species depending on PM_{2.5} concentration level.

Table 4. Frequency (days) depending on PM_{2.5} concentration level by seasons.

Period	Season	PM _{2.5} ≤ 15	15 < PM _{2.5} ≤ 30	30 < PM _{2.5} ≤ 45	45 < PM _{2.5} ≤ 60	60 < PM _{2.5}
1~2, 12.2020	Winter	560	748	480	230	165
3~5.2020	Spring	690	1027	355	82	23
6~8.2020	Summer	1180	633	247	17	1
9~11.2020	Autumn	986	679	229	76	52

3.3. Source Apportionment Using PMF Receptor Model

The correlation analysis between predicted and observed data using input data in the PMF receptor model evaluated correlation coefficients, slopes, and intercepts as all affordable values. Correlation coefficients for major components of $PM_{2.5}$, such as SO_4^{2-} , NO_3^- , NH_4^+ , OC, EC, K, and so on, indicated 0.8 or bigger values. Figure 5 shows the correlation between the predicted PMF receptor model and measurement data of $PM_{2.5}$. The correlation coefficient was 0.94. This coefficient was reasonably affordable and similar to previous studies [7].

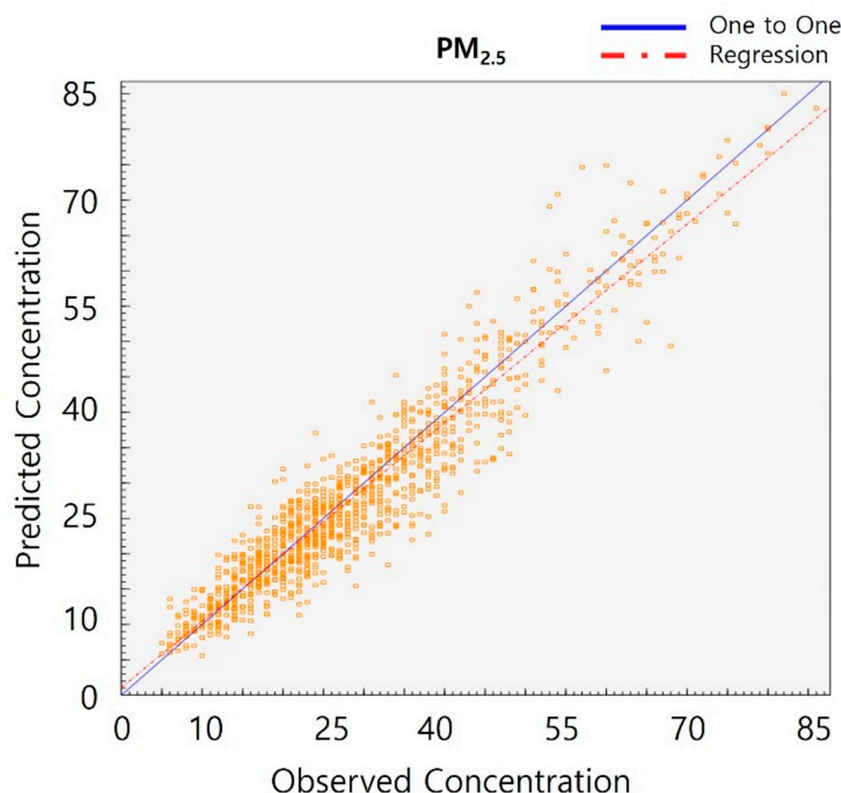


Figure 5. Scatter plot for observed and predicted $PM_{2.5}$ concentrations.

Figures 6 and 7, and Table 5, show the results of the PMF receptor model. Eight factors were determined: dust/soil, secondary nitrate, biomass burning, vehicles, secondary sulfate, industry, coal combustion, and sea salt sources. Seasonal contribution (unit: $\mu g/m^3$) for every eight sources is shown in Figure 8, i.e., spring: March to May 2020, summer: June to August 2020, autumn: September to November 2020, and winter: January to February 2020 and December 2020, respectively.

Table 5. Source contribution during the whole measurement period.

Source	Contribution
Secondary Sulfate	35%
Secondary Nitrate	26%
Vehicle	16%
Biomass burning	6%
Industry	6%
Dust/soil	6%
Sea salt	4%
Coal combustion	1%

Table 5. Cont.

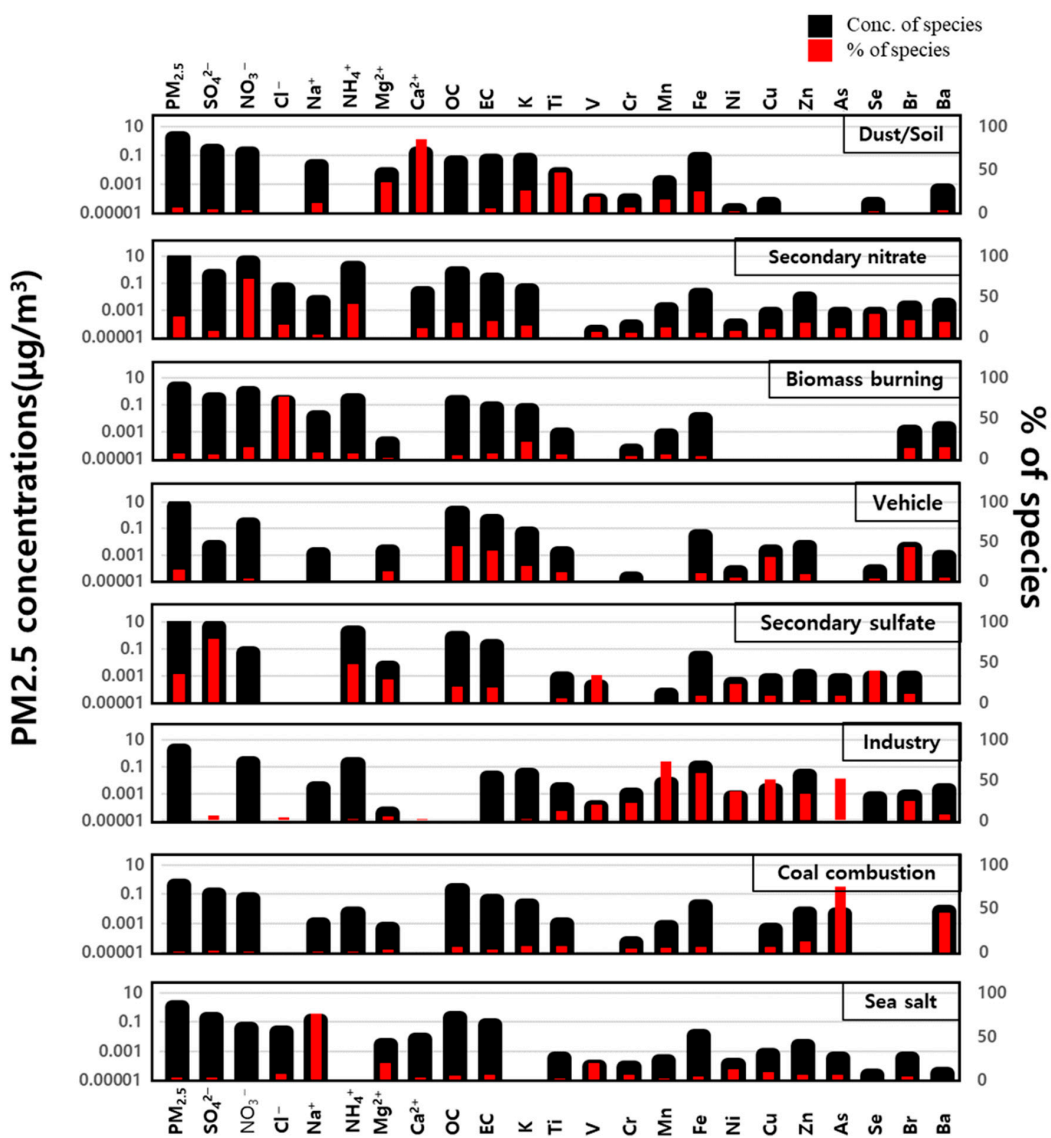
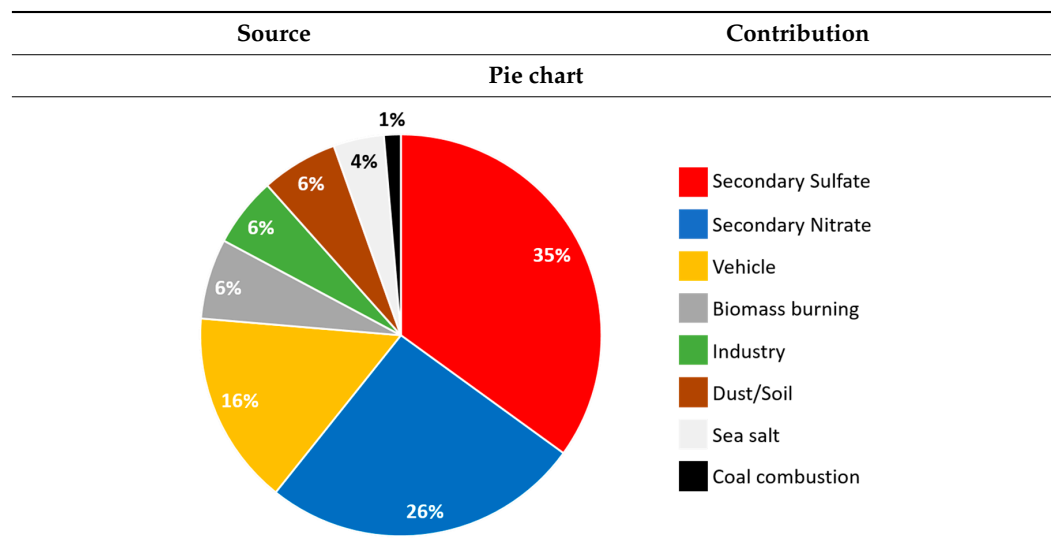


Figure 6. Factor profiles at the receptor site (Daejeon) by the PMF model.

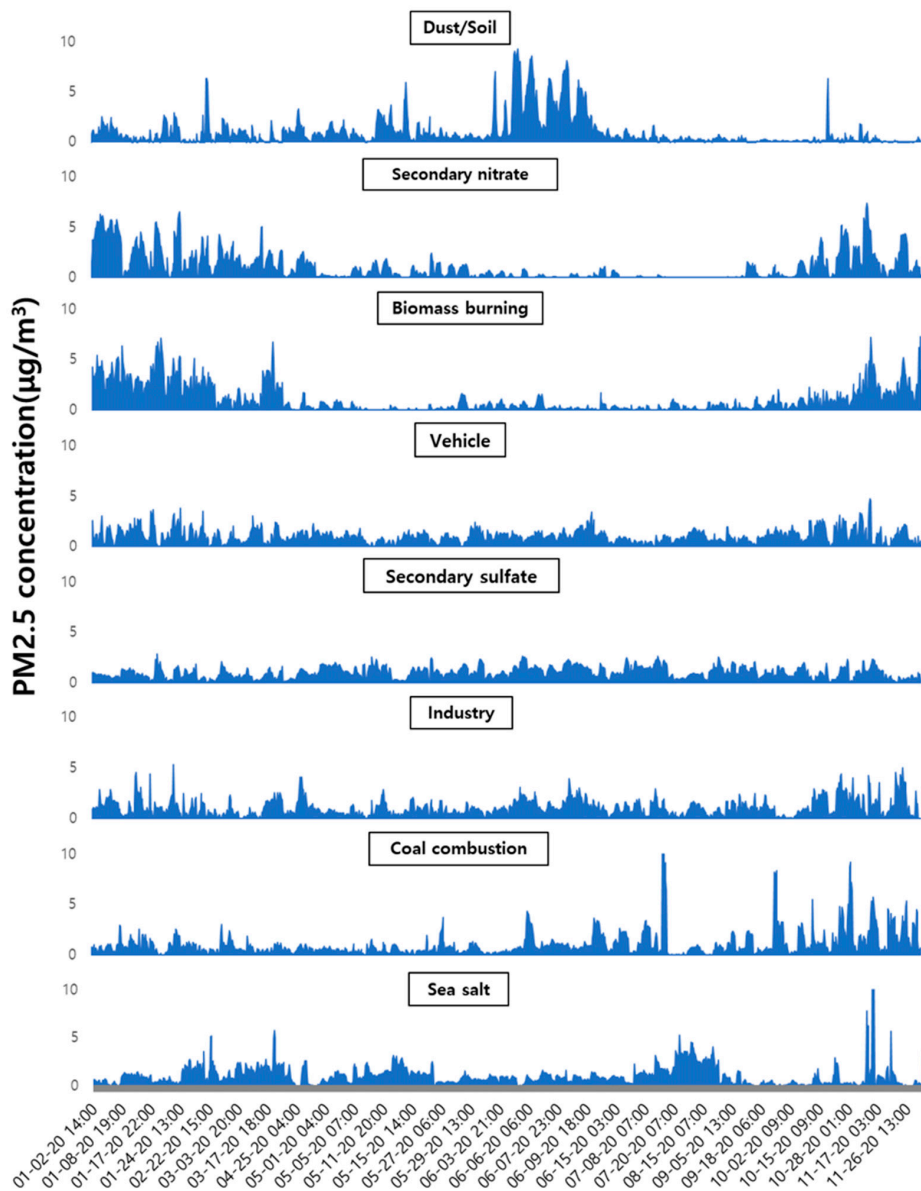


Figure 7. Factor contributions at the receptor site (Daejeon) by time series analysis.

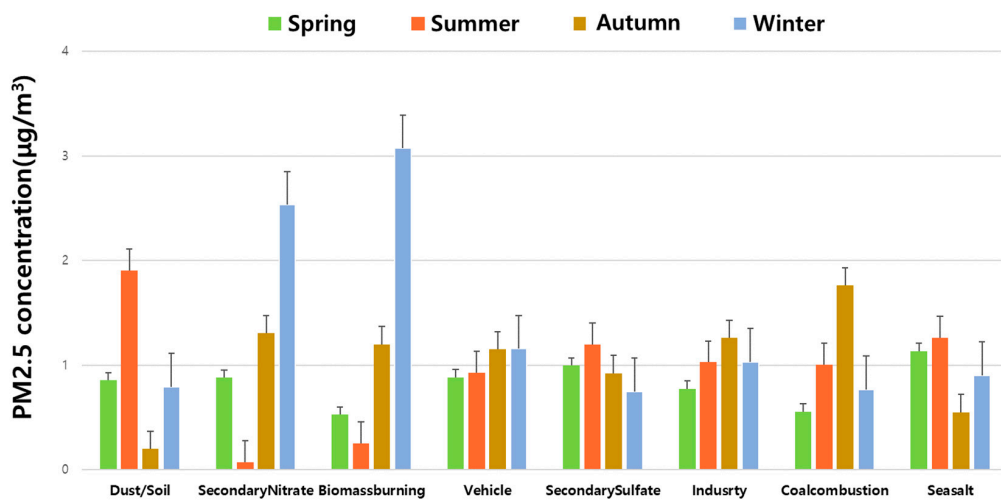


Figure 8. Seasonal contribution for each of the eight sources.

The first factor showed a high contribution of Ca^{2+} , Mg^{2+} , Ti, and Fe, and it was classified as a Dust/Soil source. The average concentration of dust was $1.73 \mu\text{g}/\text{m}^3$ (6.2%) (Table 5), and the seasonal contribution in summer was the highest (Figure 8). Similar to this study, Ca^{2+} , Mg^{2+} , Si, Ti, Fe, and Mn were used as markers for soil and dust sources in previous studies [24,31]. The second factor showed a high contribution by NO_3^- and NH_4^+ , and it was classified as a secondary nitrate source. The average concentration of this source was $7.2 \mu\text{g}/\text{m}^3$ (25.7%) (Table 5), and the seasonal contribution in the winter season was the highest (Figure 8). NO_3^- and NH_4^+ were used as markers for secondary nitrate sources [24,30,31], as similar to this study. Secondary nitrates are composed of NO_3^- and NH_4^+ , which are oxidized NO_2 combined with NH_4^+ and exist as the form of NH_4NO_3 in the atmosphere [9,32,33]. NH_4NO_3 is actively formed in the winter season by a heterogeneous reaction. Similarly, ammonia concentration was high in the winter season at 2021 Daejeon, and the formation of NH_4NO_3 was high in our previous study [30]. The third factor showed a high contribution of Cl^- and K, and it was classified as a biomass-burning source. Cl^- , K and OC were well-known as markers for biomass-burning sources [30,31]. The average concentration of this source was $1.8 \mu\text{g}/\text{m}^3$ (6.5%) (Table 5), and the seasonal contribution in the autumn and winter seasons was high (Figure 8). Biomass burning sources are frequently observed from open burnings in agricultural areas during the late fall to the winter season in Korea. The fourth factor showed a high contribution by OC, EC, and Cu, and it was classified as a vehicle source. The average concentration of this source was $4.38 \mu\text{g}/\text{m}^3$ (15.6%) (Table 5). The seasonal contribution was not significantly affected by season changes (Figure 8) and is the typical urban site pattern. Generally, OC and EC are well known as the emission species from vehicle exhaust. Previous reports show OC is high in gasoline exhaust, while EC is high in diesel exhaust [34–37]. Unfortunately, gasoline and diesel vehicles were not distinguished in this study. The fifth factor showed a high contribution of SO_4^{2-} and NH_4^+ and was classified as a secondary sulfate source. The average concentration of this source was $9.82 \mu\text{g}/\text{m}^3$ (34.9%) (Table 5), and the contribution of $\text{PM}_{2.5}$ in the Daejeon region was the highest in 8 factors. The seasonal contribution in summer was slightly higher than other seasons (Figure 8). Secondary sulfate is composed of SO_4^{2-} and NH_4^+ , which is the oxidized SO_2 combined with NH_4^+ , and it exists in the form of $(\text{NH}_4)_2\text{SO}_4$ in the atmosphere. Dockery et al. 2007 reported that high humidity and temperature influenced the conversion from SO_2 to SO_4^{2-} . Thus, the formation of $(\text{NH}_4)_2\text{SO}_4$ was more active in the summer and daytime than in the winter and nighttime seasons [7,38]. The sixth factor showed a high contribution by heavy metals such as Mn, Fe, Ni, Cu, and Zn, classified as industry sources. The average concentration of this source was $0.57 \mu\text{g}/\text{m}^3$ (5.6%) (Table 5). The seasonal contribution was not significantly affected by season changes (Figure 8) [39]. The seventh factor showed a high contribution by As, and it was classified as a coal combustion source. The average concentration of this source was $0.38 \mu\text{g}/\text{m}^3$ (1.4%) (Table 5), and the seasonal contribution in the winter season was higher compared to other seasons (Figure 8). The 8th factor showed a high contribution of Na^+ and Cl^- , which was classified as a sea salt source. Sea salt, composed of Na^+ and Cl^- , is produced from the bubbles bursting in the ocean and coast. The contribution of Cl^- was considerably low, which means that the loss of Cl^- might be caused by the reaction of HNO_3 (produced from the reaction of $\text{NH}_4\text{NO}_3 \leftrightarrow \text{HNO}_3 + \text{NH}_3$) and NaCl [40].

3.4. Results of the Regional Contributions by ACERWT

The model results between CWT and ACERWT are compared in Figure 9. Unlike the CWT result, the ACERWT model showed no contribution from the Yellow Sea region (Figure 9, left), while the CWT result showed a high contribution from the overlapping of several trajectories (Figure 9, right) [24]. This result suggests that the ACERWT model can be an alternative to overcome the limitations of the CWT model. In addition, the CWT model showed a high contribution from the near area of the receptor site and Yellow Sea regions, and the contributions of Japan and South China were low. In contrast, the ACERWT model showed a high contribution from East China and North-East China. From

the point of view of the distribution of industries and population, the result of the ACERWT model is relatively reasonable.

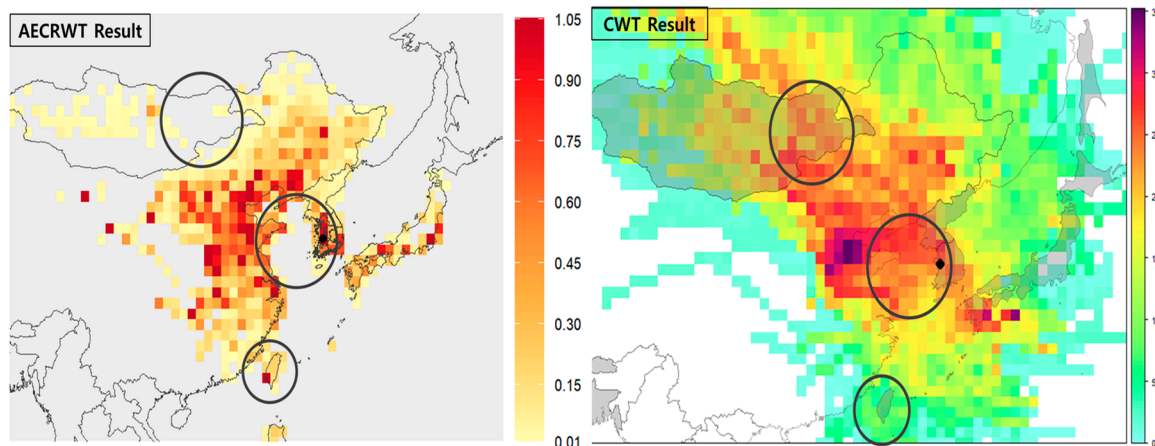


Figure 9. Comparison of ACERWT (left) and CWT (right) model results.

In the results of the ACERWT model, the regional contribution of North-Eastern China and Eastern China was the highest, followed by Southern Japan and South Korea. This result was based on the differences between back-tracking periods and emission inventories. The regional contributions by Yellow Dust were from Mongolia, a desert area in China. Filonchyk et al. (2022) mentioned that Yellow dust was produced from sandstorms in desert areas in China [41]. The contributions of eastern and south-eastern areas were high in the China region. According to Li et al.'s (2016) report, large-scale emission facilities and industrial complexes were located with a high density in Jiangsu province, Shanghai, and Henan province in Eastern China [42]. Beijing and Shanghai, i.e., China's largest metropolitan cities, have many anthropogenic emission sources in this Eastern or South-Eastern China. In the Southern Taiwan region, which contains a large harbor and the urban city of Kaohsiung, Tainan also influenced $PM_{2.5}$ pollution at the receptor site. In Japan, the regional contribution of the western area of Tokyo, Southern Japan, and Western Japan contributed to $PM_{2.5}$ pollution at the receptor site. Tokyo is the largest city in Japan, and it has the Isogo coal power plant and the Hekinan coal power plant located in the Nagoya region (Southern Japan). Goto and Kumamoto cities, with energy power plants and anthropogenic emission sources due to the high population density in those urban cities, are located in Western Japan [43].

In the domestic region, the regional contribution of Gaeseong city in North Korea is high because of the high population density and industrial complex in Gaeseong city. Moreover, the regional contribution of the Capital region (Seoul, Gyeonggi, and Incheon), Chungcheong region (Dangjin, Cheongju, and Sejong) and Gyeongsang region (Busan and Ulsan) was high; the population density of the capital region is considerably high; Gyeonggi has many industrial complexes with high density, and Incheon has a large scale of harbors and several industrial complexes. Large-scale emission sources such as the iron and steel industry and coal power plants are distributed in Dangjin; Cheongju has industrial complexes and large populations; and Sejong has a high-density population as an administrative capital. Busan and Ulsan metropolitan cities are located in the Gyeongsang region, and both cities have large-scale harbors and high populations.

4. Conclusions

In this study, we improved the hybrid receptor model using a model of Advanced Concentration, Emission, and Retention Time Weighted Trajectory (ACERWT). Using the CWT model (modified CWT model, MCWT) in our previous study, we tried to improve the limitation of the regional contribution of the hybrid receptor model caused by overlapping several air masses. The MCWT model could improve the performance of the regional

contribution model. However, it suggested further studies. Thus, we tried to use the ACERWT model combined with a Positive Matrix Factorization (PMF), the HYSPLIT (back trajectory) model and the Regional Emission Inventory. In the PMF receptor model, secondary sulfate source showed the highest contribution (35%), followed by secondary nitrate sources (26%), vehicle sources (16%), biomass burning, dust/soil and industry sources (6%, respectively), sea salt sources (5%), and coal sources (1%), respectively. The result in ACERWT showed that the limitation of the Yellow Sea impact was significantly improved in the previous studies. The contribution of the Yellow Sea to the receptor site was significantly decreased, while the contribution of China, Japan, and Korea was increased. Regions such as the eastern and south-eastern areas of China, the southern area of Taiwan, the western area of Tokyo, and the central area of Korea, which significantly showed high contributions, have large-scale emission facilities and industrial complexes. Regions of eastern and south-eastern areas of China showed a high contribution. Beijing and Shanghai, i.e., the largest metropolitan cities in China, have many anthropogenic emission sources in this eastern or south-eastern region of China. Southern Taiwan, which contains a large harbor and the urban cities of Kaohsiung and Tainan, has also highly influenced PM_{2.5} pollution at the receptor site. The regional contribution of the Western area of Tokyo, Southern Japan, and Western Japan regions influenced the regional contribution of Gaeseong city in North Korea, which was also high because of high population density and industrial complexes. This study's modified ACERWT model could estimate the regional contribution of PM_{2.5} pollution at the receptor site. The regional contribution results were reasonable, and the ACERWT model is significantly upgraded compared to the previously applied models. However, it still has a limitation for the quantitative contribution. In future studies, the improvement of the pretreatment for model application and the quantification of the regional contribution should be studied.

Author Contributions: Conceptualization, J.-s.H.; Methodology, S.-w.H. and J.-s.H.; Software, J.-s.C.; Formal analysis, S.-w.H.; Investigation, K.-j.M.; Data curation, K.-c.K.; Writing—original draft, S.-w.H.; Writing—review & editing, H.-s.J. All authors have read and agreed to the published version of the manuscript.

Funding: This research received no external funding.

Institutional Review Board Statement: Not applicable

Informed Consent Statement: Not applicable

Data Availability Statement: The data presented in this study are openly available at [<https://doi.org/10.3390/atmos13111902>], reference number [24].

Acknowledgments: This research was supported by the FRIEND (Fine Particle Research Initiative in East Asia Considering National Differences) Project through the National Research Foundation of Korea (NRF) funded by the Ministry of Science and ICT (2020M3G1A1114999) and Experts Training Graduate Program for Particulate Matter Management from the Ministry of Environment, Korea.

Conflicts of Interest: The authors declare no conflict of interest. Sang-woo Han, Jin-sik Cho are employees of E2M3 Inc. But this paper was not funded by E2M3. The company had no roles in the design of the study; in the collection, analysis, or interpretation of data; in the writing of the manuscript, or in the decision to publish the articles. The paper reflects the views of the scientists and not the company.

References

1. Jung, E.M.; Kim, K.N.; Park, H.; Shin, H.H.; Kim, H.S.; Cho, S.J.; Kim, S.T.; Ha, E.H. Association between prenatal exposure to PM_{2.5} and the increased risk of specified infant mortality in South Korea. *Environ. Int.* **2020**, *144*, 105997. [[CrossRef](#)]
2. Han, J.S.; Moon, K.J.; Kim, Y.J. Identification of potential sources and source regions of fine ambient particles measured at Gosan background site in Korea using advanced hybrid receptor model combined with positive matrix factorization. *J. Geophys. Res.* **2006**, *111*, D22217. [[CrossRef](#)]
3. Hwang, I.J.; Kim, D.S. Research trends of receptor models in Korea and Foreign Countries and Improvement Directions for Air Quality Management. *J. Korean Soc. Atmos. Environ.* **2013**, *29*, 459–476. [[CrossRef](#)]

4. Miller, M.S.; Friedlander, S.K.; Hidy, G.M. A chemical element balance for the Pasadena aerosol. *J. Colloid Interface Sci.* **1972**, *39*, 165–176. [[CrossRef](#)]
5. Paatero, P. Least squares formulation of robust non-negative factor analysis. *Chemom. Intell. Lab. Syst.* **1997**, *37*, 23–35. [[CrossRef](#)]
6. Reff, A.; Eberly, S.I.; Bhawe, P.V. Receptor modeling of ambient particulate matter data using positive matrix factorization: Review of existing methods. *J. Air Waste Manag. Assoc.* **2007**, *57*, 146–154. [[CrossRef](#)]
7. Hwang, I.; Hopke, P.K. Estimation of source apportionment and potential source locations of PM_{2.5} at a west coastal IMPROVE site. *Atmos. Environ.* **2007**, *41*, 506–518. [[CrossRef](#)]
8. Thurston, G.D.; Ito, K.; Lall, R. A source apportionment of U.S. fine particulate matter air pollution. *Atmos. Environ.* **2011**, *45*, 3924–3936. [[CrossRef](#)]
9. Belis, C.A.; Karagulian, F.; Larsen, B.R.; Hopke, P.K. Critical review and meta-analysis of ambient particulate matter source apportionment using receptor models in Europe. *Atmos. Environ.* **2013**, *69*, 94–108. [[CrossRef](#)]
10. Lu, Z.J.; Liu, Q.Y.; Xiong, Y.; Huang, F.; Zhou, J.B.; Schauer, J.J. A hybrid source apportionment strategy using positive matrix factorization (PMF) and molecular marker chemical mass balance (MM-CMB) models. *Environ. Pollut.* **2018**, *238*, 39–51. [[CrossRef](#)]
11. Park, M.B.; Lee, T.J.; Lee, E.S.; Kim, D.S. Enhancing source identification of hourly PM_{2.5} data in Seoul based on a dataset segmentation scheme by positive matrix factorization (PMF). *Atmos. Pollut. Res.* **2019**, *10*, 1042–1059. [[CrossRef](#)]
12. Park, J.E.; Kim, H.W.; Kim, Y.K.; Heo, J.B.; Kim, S.W.; Jeon, K.H.; Yi, S.M.; Hopke, P.K. Source apportionment of PM_{2.5} in Seoul, South Korea and Beijing, China using dispersion normalized PMF. *Sci. Total Environ.* **2022**, *833*, 155056. [[CrossRef](#)]
13. Hopke, P.K.; Gao, N.; Cheng, M.D. Combining chemical and meteorological data to infer source areas of airborne pollutants. *Chemom. Intell. Lab. Syst.* **1993**, *19*, 187–199. [[CrossRef](#)]
14. Seibert, P.; Kromp-Kolb, H.; Baltensperger, U.; Jost, D.T.; Schwikowski, M.; Kasper, A.; Puxbaum, H. Trajectory analysis of aerosol measurements at high Alpine sites. In *Transport and Transformation of Pollutants in the Troposphere*; Borrell, P.M., Ed.; Elsevier: New York, NY, USA, 1994; Volumes 689–693.
15. Stohl, A. Trajectory statistics—A new method to establish source-receptor relationships of air pollutants and its application to the transport of particulate sulfate in Europe. *Atmos. Environ.* **1996**, *30*, 579–587. [[CrossRef](#)]
16. Han, Y.J.; Holsen, T.M.; Hopke, P.K.; Cheong, J.P.; Kim, H.; Yi, S.M. Identification of source locations for atmospheric dry deposition of heavy metals during yellow-sand events in Seoul, Korea in 1998 using hybrid receptor models. *Atmos. Environ.* **2004**, *38*, 5353–5361. [[CrossRef](#)]
17. Lupu, A.; Maenhaut, W. Application and comparison of two statistical trajectory techniques for identification of source regions of atmospheric aerosol species. *Atmos. Environ.* **2002**, *36*, 5607–5618. [[CrossRef](#)]
18. Fan, W.; Qin, K.; Xu, J.; Yuan, L.; Li, D.; Jin, Z.; Zhang, K. Aerosol vertical distribution and sources estimation at a site of the Yangtze River Delta region of China. *Atmos. Res.* **2019**, *217*, 128–136. [[CrossRef](#)]
19. Dimitriou, K.; Mihalopoulos, N.; Leeson, S.R.; Twigg, M.M. Sources of PM_{2.5}-bound water soluble ions at EMEP's Auchencorth Moss (UK) Supersite revealed by 3D-Concentration Weighted Trajectory (CWT) model. *Chemosphere* **2021**, *274*, 129979. [[CrossRef](#)]
20. Wang, Y.Q.; Zhang, X.Y.; Arimoto, R. The contribution from distant dust sources to the atmospheric particulate matter loadings at XiAn, China during spring. *Sci. Total Environ.* **2006**, *368*, 875–883. [[CrossRef](#)]
21. Jeong, U.K.; Kim, J.H.; Lee, H.L.; Jung, J.S.; Kim, Y.J.; Song, C.H.; Koo, J.H. Estimation of the contributions of long range transported aerosol in East Asia to carbonaceous aerosol and PM concentrations in Seoul, Korea using highly time resolved measurements: A PSCF model approach. *J. Environ. Monit.* **2011**, *13*, 1905–1918. [[CrossRef](#)]
22. Zachary, M.; Yin, L.; Zacharia, M. Application of PSCF and CWT to Identify Potential Sources of Aerosol Optical Depth in ICIPE Mbita. *Open Access Libr. J.* **2018**, *5*, e4487. [[CrossRef](#)]
23. Do, W.G.; Jung, W.S. Estimation of PM₁₀ source locations in Busan using PSCF model. *J. Environ. Sci. Int.* **2015**, *24*, 793–806. [[CrossRef](#)]
24. Han, S.; Joo, H.; Song, H.; Lee, S.; Han, J. Source apportionment of PM_{2.5} in Daejeon metropolitan region during January and May to June, 2021 in Korea using a hybrid receptor model. *Atmosphere* **2022**, *13*, 1902. [[CrossRef](#)]
25. National Institute of Environmental Research (NIER). *Annual Report of Intensive Air Quality Monitoring Station*; NIER: Incheon, Republic of Korea, 2020; NIER-GP2020–2208.
26. Nuhoglu, Y.; Yazici, M.; Nuhoglu, C.; Kam, E.; Adar, E.; Kuzu, L.; Osmanlioglu, A.E. XRF Analysis of Airborne Heavy Metals and Distribution of Environment in Sivas City Turkey through Dust Samples. In *Proceedings of the EurAsia Waste Management Symposium, Istanbul, Turkey, 26–28 October 2020*; pp. 26–28.
27. National Institute of Environmental Research (NIER). *Establishment of Guidelines for the PMF Modeling and Applications*; NIER: Incheon, Republic of Korea, 2020; NIER-SP2020–2273.
28. Kurokawa, J.; Ohara, T. Long-Term Historical Trends in Air Pollutant Emissions in Asia: Regional Emission Inventory in Asia (REAS) version 3. *Atmos. Chem. Phys.* **2020**, *20*, 12761–12793. [[CrossRef](#)]
29. Guo, S.; Hu, M.; Wang, Z.B.; Slanina, J.; Zhao, Y.L. Size-resolved aerosol water-soluble ionic compositions in the summer of Beijing: Implication of regional secondary formation. *Atmos. Chem. Phys.* **2010**, *10*, 947–959. [[CrossRef](#)]
30. National Research Foundation of Korea (NRF). A study on the physicochemical properties and formation mechanism considering the characteristics of domestic and foreign influences of fine particles in the central area. In *Fine Particle Research Initiative in East Asian Considering National Differences (FRIEND) Project, 2020MG1A1114999*; National Research Foundation of Korea (NRF): Daejeon, Republic of Korea, 2022.

31. Hwang, I.J.; Yi, S.M.; Park, J.S. Estimation of Source Apportionment for Filter-based PM_{2.5} Data using the EPA-PMF Model at Air Pollution Monitoring Supersites. *J. Korean Soc. Atmos. Environ.* **2020**, *36*, 620–632. [[CrossRef](#)]
32. Taghvaei, S.; Sowlat, M.H.; Mousavi, A.; Hassanvand, M.S.; Yunesian, M.; Naddafi, K.; Sioutas, C. Source apportionment of ambient PM_{2.5} in two locations in central Tehran using the Positive Matrix Factorization (PMF) model. *Sci. Total Environ.* **2018**, *628–629*, 672–686. [[CrossRef](#)]
33. Chun, M.Y.; Lee, Y.J.; Kim, H.K. Concentration of NH₄NO₃ in TSP in Seoul Ambient Air. *J. Korean Soc. Atmos. Environ.* **1994**, *10*, 130–136.
34. Bayramoğlu Karşı, M.B.; Berberler, E.; Berberler, T.; Aslan, Ö.; Yenisoy-Karakaş, S.; Karakaş, D. Correction and source apportionment of vehicle emission factors obtained from Bolu Mountain Highway Tunnel, Turkey. *Atmos. Pollut. Res.* **2020**, *11*, 2133–2141. [[CrossRef](#)]
35. Hao, Y.; Gao, C.; Deng, S.; Yuan, M.; Song, W.; Lu, Z.; Qiu, Z. Chemical characterisation of PM_{2.5} emitted from motor vehicles powered by diesel, gasoline, natural gas, and methanol fuel. *Sci. Total Environ.* **2019**, *674*, 128–139. [[CrossRef](#)]
36. Coufalík, P.; Matoušek, T.; Křůmal, K.; Vojtišek-Lom, M.; Beránek, V.; Mikuška, P. Content of metals in emissions from gasoline, diesel, and alternative mixed biofuels. *Environ. Sci. Pollut. Res. Int.* **2019**, *26*, 29012–29019. [[CrossRef](#)]
37. Cheung, K.L.; Ntziachristos, L.; Tzamkiozis, T.; Schauer, J.J.; Samaras, Z.; Moore, K.F.; Sioutas, C. Emissions of particulate trace elements, metals and organic species from gasoline, diesel, and biodiesel passenger vehicles and their relation to oxidative potential. *Aerosol Sci. Technol.* **2010**, *44*, 500–513. [[CrossRef](#)]
38. Dockery, D.W.; Stone, P.H. Cardiovascular risks from fine particulate air pollution. *N. Engl. J. Med.* **2007**, *356*, 511–513. [[CrossRef](#)]
39. Son, S.E.; Park, S.S.; Bae, M.A.; Kim, S.T. A study on characteristics of high pollution observed around large scale stationary sources in Chungcheongnam-do province. *J. Korean Soc. Atmos. Environ.* **2020**, *36*, 669–687. [[CrossRef](#)]
40. Gonçalves, S.J.; Weis, J.; China, S.; Evangelista, H.; Harder, T.H.; Müller, S.; Sampaio, M.; Laskin, A.; Gilles, M.K.; Godoi, R.H.M. Photochemical reactions on aerosols at West Antarctica: A molecular case-study of nitrate formation among sea salt aerosols. *Sci. Total Environ.* **2021**, *758*, 143586. [[CrossRef](#)]
41. Filonchyk, M.; Peterson, M. Development, progression, and impact on urban air quality of the dust storm in Asia in March 15–18, 2021. *Urban Clim.* **2022**, *41*, 101080. [[CrossRef](#)]
42. Li, Y.; Lin, T.; Hu, L.; Feng, J.; Guo, Z. Time trends of polybrominated diphenyl ethers in east China seas: Response to the booming of PBDE pollution industry in China. *Environ. Int.* **2016**, *92–93*, 507–514. [[CrossRef](#)]
43. Garcia Novo, P.; Kyoizuka, Y. Tidal stream energy as a potential continuous power producer: A case study for west Japan. *Energy Convers. Manag.* **2021**, *245*, 114533. [[CrossRef](#)]

Disclaimer/Publisher’s Note: The statements, opinions and data contained in all publications are solely those of the individual author(s) and contributor(s) and not of MDPI and/or the editor(s). MDPI and/or the editor(s) disclaim responsibility for any injury to people or property resulting from any ideas, methods, instructions or products referred to in the content.